J. exp. Biol. **114**, 259–284 (1985)
Printed in Great Britain © *The Company of Biologists Limited 1985*

MECHANICAL PROPERTIES OF THE OCTOPUS AORTA

BY ROBERT E. SHADWICK AND JOHN M. GOSLINE

Department of Zoology, University of British Columbia, Vancouver, B.C., Canada

Accepted 6 July 1984

SUMMARY

The quasi-static mechanical properties of the aorta of *Octopus dofleini* were investigated using biaxial inflation and uniaxial force-extension tests on vessel segments *in vitro*. The octopus aorta is a highly compliant and non-linearly elastic structure. The elastic modulus (i.e. the stiffness) measured circumferentially (E_C) and longitudinally (E_L) increased markedly with distension of the vessel wall. E_C was always greater than E_L, and varied from about 10^4 to 2×10^5 N m^{-2} between 2 and 5 kPa pressure respectively, the approximate range of resting blood pressure in this species. Increasing vessel wall stiffness is necessary for the aorta to be compliant at low pressure, and at the same time to be protected from 'blowout' at high pressure. The non-linear elasticity of the octopus aorta at physiological pressures can be attributed to the properties of the rubber-like elastic fibres which are present in the vessel wall, with little contribution from stiff collagen fibres being required until very high pressures. Dynamic mechanical properties of the aorta were measured by the method of forced oscillations. The dynamic modulus in the circumferential direction increased continuously to almost twice the static value as the frequency was raised from 0·05 to 10 Hz. At the same time, the viscous damping, tan δ, increased from 0·11 to 0·27. The resilience of the octopus aorta was close to 70 % at the relevant physiological frequencies. We conclude that this vessel is suitably designed to function as an efficient elastic energy storage component in the octopus circulatory system.

INTRODUCTION

Investigations on the mechanical properties of blood vessels have been numerous since Roy (1880) first gave a detailed quantitative description of the long-range elastic behaviour of the mammalian aorta. He showed that this vessel was very distensible at physiological pressure, but became much less distensible as the pressure was increased. Roy demonstrated two other important properties of arteries: that inflation was accompanied by viscous energy losses, and that the artery wall was thermodynamically similar to natural rubber.

More recent studies have added considerable detail to these fundamental observations (for reviews see Dobrin, 1978; Cox, 1979). We now know that the

Key words: Mechanical properties, viscoelasticity, aorta, octopus.

mammalian artery wall has non-linear elastic properties which arise from a complex arrangement of two fibrous connective tissue proteins: elastin, which is highly extensible and rubber-like, and collagen, which is stiff and relatively inextensible. At low physiological pressures the artery wall is highly compliant, as the pressure is resisted largely by the elastin. With increasing pressures in the physiological range and above, the artery wall becomes much stiffer due to mechanical recruitment of more elastin fibres and finally, to the transfer of load to the collagen network.

The role of the arteries as a passive elastic component in the high pressure closed circulatory system of mammals is well established (McDonald, 1974). In addition to being blood conduits, large arteries are important in reducing the pulsatility of blood flow from the heart to the body tissues. The arteries are distended with blood during systole, while passive elastic recoil provides continued flow during diastole. The elasticity of the large arteries is an important determinant of the dynamics of blood flow in the cardiovascular systems of mammals (McDonald, 1974) as well as other vertebrates (Speckman & Ringer, 1966; Satchell, 1971; Langille & Jones, 1975, 1977; Burggren, 1977).

Until recently there were no reports in the literature on the mechanical properties of blood vessels from any invertebrate animal. This was not surprising since most invertebrates have relatively simple, open circulatory systems. However, in cephalopods the vascular system has attained a high level of complexity; the system is closed, and has an extensive network of blood vessels and capillaries (Wells, 1978; Browning, 1980). Observations on blood pressures in the octopus (Johansen & Martin, 1962; Wells, 1979), nautilus (Bourne, Redmond & Johansen, 1978) and squid (Bourne, 1982) suggested that the large arteries function as elastic reservoirs in these animals. We measured the mechanical properties of the aorta of several species of cephalopod, and found that these vessels were indeed highly extensible elastic structures (Shadwick & Gosline, 1981; Gosline & Shadwick, 1982). We also showed previously that the octopus aorta contains a connective tissue network made up of a protein with rubber-like properties. We proposed that this protein provides the long-range elasticity in the octopus vessel wall, and thus is a functional analogue of elastin (Shadwick & Gosline, 1985).

In this paper we present a quantitative analysis of the non-linear and viscoelastic properties of the octopus aorta *in vitro*. Our results indicate that this vessel is mechanically similar to the major arteries of vertebrates, and is suitably designed to function as an efficient elastic energy storage element in the circulatory system. We also demonstrate that the elastic properties of the artery wall at physiological pressure can be attributed to the presence of the rubber-like protein which we have called the octopus arterial elastomer (OAE).

THEORETICAL BACKGROUND

Non-linear elasticity in thick-walled tubes

Materials with linear (Hookean) elasticity can be characterized by a constant called the Young's modulus of elasticity. This is defined as stress (σ) divided by strain (ϵ), where stress is the force divided by the cross-sectional area over which the

force is applied, and strain is the ratio of the change in length to the initial length. Extensible biological tissues like artery wall typically have non-linear stress-strain relationships. Therefore, the elastic modulus is not a constant, but is dependent on the level of strain. For these materials we can define a tangential modulus of elasticity (E), for each strain, as the slope of the stress-strain curve at that strain.

$$E = \Delta\sigma/\Delta\epsilon. \tag{1}$$

This equation applies only to stress-strain data obtained from the extension (or compression) of a material in a single direction by a linearly applied force. The mechanical properties of arteries can be measured *in vitro* by uniaxial tests on strips or ring slices, and equation 1 may be used. However, it is more desirable to use inflation tests on intact vessel segments in order to mimic more closely the *in vivo* situation. Consider a thick wall elastic tube at equilibrium with a distending pressure P, (Fig. 1). There will be tensile forces in two perpendicular directions simultaneously, circumferential and longitudinal. There will also be a compressive force acting radially, but since this will be relatively small (Dobrin, 1978) it is ignored

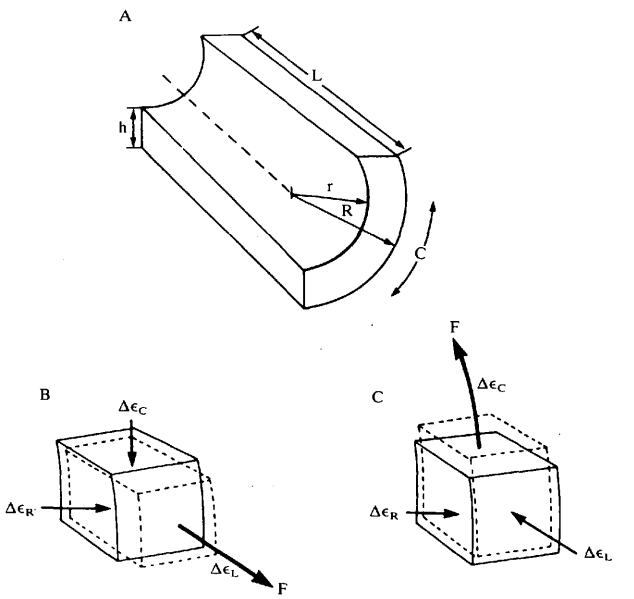

Fig. 1. (A) Diagram of an arterial segment to define the circumferential (C) and longitudinal (L) directions. R is the outside radius, r is the inside radius, and h is the wall thickness. (B) Diagram to illustrate Poisson's ratios. A uniaxial force (F) in the longitudinal direction causes decreases in the circumferential and radial directions. (C) A uniaxial force in the circumferential direction causes decreases in the longitudinal and radial directions (after Dobrin, 1978).

here in order to simplify our analysis. The circumferential stress in the wall (σ_C) is given by:

$$\sigma_C = Pr/h, \tag{2}$$

where r is the inside radius and h is the vessel wall thickness. Strain in the circumferential direction is calculated at the mid-wall radius as:

$$\epsilon_C = \Delta\tilde{R}/\tilde{R}_0, \tag{3}$$

where $\tilde{R} = (R+r)/2$, R is the outside radius and $\tilde{R}_0$ is the unstressed mid-wall radius. Stress in the longitudinal direction (σ_L) is given by:

$$\sigma_L = Pr^2/2\tilde{R}h. \tag{4}$$

As R/h increases, R approaches r and σ_L approaches $\sigma_C/2$ (i.e. in a thin wall tube the circumferential stress is twice the longitudinal stress). Longitudinal strain (ϵ_L) is given as:

$$\epsilon_L = \Delta L/L_0, \tag{5}$$

where L_0 is the unstressed vessel segment length.

When an artery is pressurized it is loaded biaxially, and the relationships between stress, strain and modulus become more complex than the one given by equation 1. For example, a pressure increment gives a strain in the circumferential direction which depends on the stress and the elastic modulus in that direction, but which also depends on the strain increment which occurs simultaneously in the longitudinal direction. The interaction between pairs of orthogonal strains in a material is described by the Poisson's ratio (ν). If the artery wall is incompressible and mechanically anisotropic (i.e. the longitudinal modulus E_L is not equal to the circumferential modulus E_C) at least two Poisson's ratios are necessary to describe the relationship between ϵ_C and ϵ_L. These are defined as:

$$\nu_{CL} = -\Delta\epsilon_C/\Delta\epsilon_L \tag{6}$$

and

$$\nu_{LC} = -\Delta\epsilon_L/\Delta\epsilon_C, \tag{7}$$

where ν_{CL} is the ratio of circumferential to longitudinal strains when the artery is subjected to a longitudinal stress only (Fig. 1B) and ν_{LC} is the ratio of longitudinal to circumferential strains when the structure is subjected to a circumferential stress only (Fig. 1C). Values of ν should vary between 0 and 1·0. The Poisson's ratios are related to the elastic moduli as follows:

$$\nu_{LC}/E_C = \nu_{CL}/E_L. \tag{8}$$

When an artery is inflated the increase in circumference will tend to decrease the vessel length, while at the same time, the pressure will tend to increase the length. Whether the artery actually lengthens or shortens, and by how much, is dependent on the Poisson's ratios and the relative values of the elastic moduli. Dobrin & Doyle (1970) described a method for estimating these parameters from inflation tests. For a given pressure increment, the two simultaneous strain increments are given as:

$$\Delta\epsilon_L = (\Delta\sigma_L/E_L) - \nu_{CL}(\Delta\sigma_C/E_L) \tag{9}$$

and

$$\Delta\epsilon_C = (\Delta\sigma_C/E_C) - \nu_{CL}(\Delta\sigma_L/E_L). \tag{10}$$

Comparison with equation 1 shows that the biaxial strains are less than uniaxial strains by an amount which depends on ν. Clearly, then, the slope of the biaxial stress-strain curve is not a direct measure of E. The analysis using equations 9 and 10 is based on the assumptions that radial stresses are small enough to ignore, shearing stresses do not occur and the artery wall is incompressible. The first two assumptions greatly simplify the mathematics involved. The incompressibility assumption is useful because if the volume of a vessel segment is known, then measurement of two of its dimensions allows calculation of the third dimension.

Viscoelastic behaviour and incremental elasticity

We have considered the artery wall as an elastic structure for which the mechanical response is independent of the rate of deformation. In reality, biological materials exhibit time-dependent elasticity because they have properties both of elastic solids and viscous fluids. A perfectly elastic solid deforms instantly under a given stress to a constant strain. Removal of the stress is followed by instantaneous recovery of the original dimensions because all the work done in deformation is stored as elastic energy and can be recovered without loss. On the other hand, a stress applied to a purely viscous fluid will cause deformation at a constant strain rate, determined by the viscosity. Energy used to drive viscous flow is lost as heat. The response of a viscoelastic material to stress or strain will be between these two extremes, depending on the relative contribution of the elastic and viscous components (Wainwright, Biggs, Currey & Gosline, 1976). There are several ways to quantify viscoelastic properties of arteries *in vitro*. One method is by dynamic mechanical testing over a range of frequencies. This technique provides a direct measure of viscoelasticity in a form that can be related to haemodynamic parameters such as pulse wave velocity and vascular impedance. Arteries *in vivo* are subjected to a static stress arising from the mean blood pressure, and a dynamic stress applied by the pressure pulse from each heartbeat. To simulate these conditions *in vitro* a small sinusoidal strain oscillation is imposed upon a static load, and the resulting stress oscillation is observed at each frequency. If the material exhibits linear viscoelasticity the stress will also be sinusoidal and will be phase shifted ahead of the strain by an angle δ. The magnitude of δ indicates the relative importance of viscosity to the overall mechanical response of the material. In theory, δ may vary from 0° for pure elasticity to 90° for pure viscosity.

It is appropriate to describe dynamic elasticity in arteries by using a strain increment (ϵ_{inc}) based on the mean radius at which the increment occurs, ($\hat{R}$), rather than the unpressurized radius (Bergel, 1961*a*, 1972; McDonald, 1974):

$$\epsilon_{inc} = \Delta R/\hat{R}. \tag{11}$$

For uniaxial tests we can define a dynamic incremental elastic modulus as:

$$E^* = \Delta\sigma/\epsilon_{inc} = (1+\epsilon)\,\Delta\sigma/\Delta\epsilon. \tag{12}$$

Note that E^* is related to the tangent modulus E by the factor $(1+\epsilon)$, since $\hat{R} = R_0(1+\epsilon)$. E^* could also be calculated from oscillatory inflation data by substituting ϵ_{inc} for $\Delta\epsilon$ in equations 9 and 10. An alternative and easier calculation of E^* from dynamic inflation data is possible if the change in length which accompanies the circumferential strain increment is zero, or negligibly small (Bergel, 1961*a*). Under these conditions,

$$E^* = (1-\nu^2)\,\Delta\sigma/\epsilon_{inc} = (1+\epsilon)(1-\nu^2)\,\Delta\sigma/\Delta\epsilon. \tag{13}$$

E^* can be resolved into two components (Ferry, 1970). E', the storage modulus, is derived from the component of stress which is in phase with the strain, and is proportional to the energy stored elastically in each cycle. E'', the loss modulus, represents the out-of-phase component of stress and is proportional to the viscous energy lost per cycle. E' and E'' are determined from measured values of E^* and δ.

$$E' = E^*(\cos\delta) \tag{14}$$

and

$$E'' = E^*(\sin\delta). \tag{15}$$

The loss angle is often expressed by the tangent ($\tan\delta = E''/E'$). Tan δ is an indication of the amount of energy lost relative to the energy stored per cycle. The analysis is based on a linear viscoelastic model, which is not adequate to describe the non-linear behaviour of blood vessels over large extensions. However, if the strain oscillations are sufficiently small so that the stress response is almost linear, then equations 14 and 15 can be used to separate the elastic and viscous components of E^* for each frequency (Fung, 1981).

METHODS

Live specimens of *Octopus dofleini*, 10–15 kg in weight, were obtained from the waters of Puget Sound, Washington, and Barkley Sound, British Columbia. The animals were maintained in good health in a recirculating sea water system at 10 °C, and fed on fish, crabs and clams.

Experiments were performed on segments of the dorsal aorta, the major vessel which leaves the systemic heart. Aortae were dissected from animals which had been

anaesthetized by chilling and killed by decerebration. The samples were washed and kept at 4 °C in saline (0·4 μm filtered sea water) containing 1 % of a solution of penicillin, streptomycin and fungizone (Gibco Labs), and used for mechanical tests within 12 h of death. These tests were at 10 °C, or in some cases at room temperature (20 °C). No differences in the passive mechanical response of the aortae could be detected between these temperatures.

Inflation experiments

Artery segments about 5 cm long were cannulated at one end with a tubular metal connector of appropriate diameter and held in the saline-filled chamber. This connector was linked to a saline pressure reservoir and either a linear infusion pump for quasi-static tests or a sinusoidal pump for dynamic tests. After saline perfusion to clear air bubbles from the system, the distal end of the specimen was ligated. This arrangement left the artery free to lengthen as it was inflated. Most samples of aorta were taken between the heart and the digestive gland where no branch vessels were present (see Wells, 1983). In some cases a more distal portion of the aorta at about the level of the crop was used, and branch vessels were ligated. Leak-free preparations were normally obtained without difficulty.

Quasi-static pressure-volume curves were generated by very slow, continuous cycles of inflation and deflation of the vessel segment by the linear pump. The pump consisted of a calibrated glass syringe with a spring-loaded piston which could be advanced or retracted at a predetermined rate by a reversible, variable-speed motor (Cole-Parmer Master Servo-Dyne). A cycle consisted of taking the artery from zero pressure to about 10 kPa (=100 cmH_2O) and back to zero. The cycles were repeated until stable P-V curves were obtained. Infusion rates were varied from 10 to 15 $\mu l\,s^{-1}$, depending on the specimen size, so that each cycle took 2 to 3 min. For a typical unpressurized specimen $r = 0{\cdot}12$ cm, $R = 0{\cdot}23$ cm and $L = 3{\cdot}5$ cm. A preconditioning period consisting of several inflation cycles was required in order to obtain stable P-V curves.

Transmural pressure was measured through an 18 gauge needle which was glued into the artery connector and coupled to a BioTec BT70 pressure transducer by a short length of polyethylene tubing (PE 190). Changes in the external diameter or length of the artery were determined with a video measuring system. This consisted of a video dimension analyser (Instruments for Medicine and Physiology VDA 303) that provides an analogue voltage which is proportional to the distance between two reference points in the video image. The dimension measurement is made on the horizontal axis of the television and the resolution is about 0·1 % of the full width of the screen (Fung, 1981).

Experiments to demonstrate the effect of vascular muscle activation on the mechanical behaviour of the artery wall were carried out using 5-hydroxytryptamine (5-HT-creatine sulphate complex, Sigma Co.) to stimulate and acetylcholine (ACh-chloride, Sigma Co.) to relax the muscles. The drugs were dissolved in saline and introduced into the artery lumen by infusion after opening the distal ligature. As the drug solution flowed through the vessel it was allowed to mix into the surrounding bath. The ligature was then closed and the artery was inflated, using the same drug solution in the pump.

Dynamic inflation experiments involved measuring small pressure and diameter oscillations over a frequency range of 0·05 to 10 Hz. These experiments were carried out on artery segments at three different mean pressures: 3, 4 or 6 kPa (corresponding to circumferential strains of approximately 0·6, 1·0, 1·2 respectively). Small sinusoidal volume changes were imposed on the inflated artery by a diaphragm pump driven by an electromagnetic vibrator (Ling Systems 200). The amplitude and frequency of the vibrator were controlled by a signal generator which also provided the frequency reference for a phase analyser. A needle valve inserted between the pump and the static pressure head ensured that flow from the pump back into the reservoir would be negligible. The volume amplitude was adjusted to give diameter changes of less than ±5 % of the mean value. Under these conditions the pressure (P) and diameter (D) oscillations were sinusoidal with little distortion, and P-D hysteresis loops were essentially linear. The amplitudes and the phase shift (δ) between P and D signals at each frequency were measured by the phase analyser (SE Labs SM272DP Transfer Function Analyser) as described by Denny & Gosline (1980). The P and D signals were also recorded continuously on a two-channel strip chart recorder.

The frequency response characteristics of the pressure transducer were tested by a free-vibration method using a step function of pressure ('pop' test, Gabe, 1972). The transducer and tubing together had a damped resonant frequency of 45 Hz, and a damping factor of 0·26. Over the frequency range used the pressure signal was delayed by 0·7° per Hz, and had an amplitude error of less than 4 % at 10 Hz. The VDA output is processed through an internal single RC 15 Hz filter, which at 10 Hz gives a 25 % attenuation and a 135° phase lag. The frequency response of the VDA over the relevant frequencies was measured with the phase analyser. Appropriate corrections for phase and amplitude losses were made to the pressure and diameter data.

After each inflation experiment the unstressed length and external radius were recorded. The thickness of the vessel wall was measured on frozen-cut transverse sections, using a microscope micrometer. The vessel wall volume was calculated on the basis of uniform cylindrical geometry and assuming isovolumetric deformation. This allowed us to determine vessel length L, and inside radius r, from V and R at any pressure, or R and r from V and L. Equations 2–5 were used to obtain biaxial stress-strain curves. Values of tangential elastic moduli were computed from equations 9 and 10 by the method of Dobrin & Doyle (1970). Dynamic pressure and radius data were used with equation 13 to obtain values of the dynamic incremental elastic modulus in the circumferential direction.

Uniaxial force-extension tests

Quasi-static uniaxial tests of the aorta were carried out on a tensile testing machine (Instron model 1120). Short transverse sections of aorta (3–4 mm long) were mounted over two rigid L-shaped stainless steel bars, one of which was secured to the base of the test frame, while the other one was attached to a force transducer on the moveable cross-head of the Instron. This transducer gave reliable measurements of forces from about 0·1 to 500 g. Force-extension tests were conducted by slow cyclic stretching at constant rates from 0·5 to 5 mm min^{-1} (i.e. strain rates of 0·002

to $0{\cdot}02\,s^{-1}$). No differences in the response of the artery specimens were detected over the range of strain rates used. Extension of the sample was determined from the cross-head displacement. Data were recorded on an X-Y plotter. Since the ring samples became flattened under a force of less than 1 g, they were considered to be two parallel sheets of tissue, each having a length equal to one-half of the circumference of the ring. Thus uniaxial extension of ring samples resulted in stresses which were essentially in the circumferential direction (Attinger, 1968; Goedhard & Knoop, 1973). Preconditioning of the samples was achieved by repeated strain cycling until relatively stable force-extension curves were obtained. During the experiments the samples were immersed in a saline bath at 10 °C.

In another series of experiments the longitudinal elastic properties of the aorta were investigated. Vessel segments about 5 cm long were mounted in the saline bath by ligating the ends over tubular connectors which were attached to the Instron test frame. Longitudinal force-extension tests were done according to the procedure described for the ring samples. A hole through one connector allowed fluid movement in and out of the vessel lumen, thus maintaining the transmural pressure at zero throughout the test.

Sample dimensions were measured at the end of each test. Strain calculations were based on an unstressed sample length which was measured at the crosshead position where a positive force was just detectable. Stress was calculated as the force divided by the cross-sectional area of the specimen, which for rings was taken as 2hL (see Fig. 1A), while for the longitudinal samples it was $\pi(R^2-r^2)$. With the assumption of isovolumetric deformation of the artery wall, the cross-sectional area, and thus the stress, at each strain could be calculated from the initial dimensions.

Dynamic mechanical tests were conducted on artery ring samples by using a forced strain oscillation technique which was analogous to the dynamic inflation. Ring samples were loaded to predetermined strains and then subjected to small sinusoidal strain increments at 0·1–10 Hz, by an electromagnetic vibration apparatus (Gosline & French, 1979). Deformation of the sample was measured by a strain gauge displacement transducer attached to the vibrator shaft. Force was measured by a semiconductor strain gauge transducer which was linked, by the sample, to the vibrator. Experiments were performed at mean strains of 0·3 and 0·6. The displacement amplitude was kept small enough (±2 % of the mean strain) to give relatively linear force-extension hysteresis loops. Force and displacement signals were conditioned with matched carrier amplifiers (SE Labs type 4300), and the amplitudes and phase relationship measured by the Transfer Function Analyser. The resonant frequency of the force transducer was two orders of magnitude greater than the highest test frequency and therefore no signal corrections were necessary. The force and extension data were used to calculate the dynamic incremental modulus, according to equation 12.

RESULTS

Inflation experiments

The first four consecutive inflation cycles for an aortic segment are shown in Fig. 2. The first inflation curve is highly sigmoid and lies well above the deflation curves.

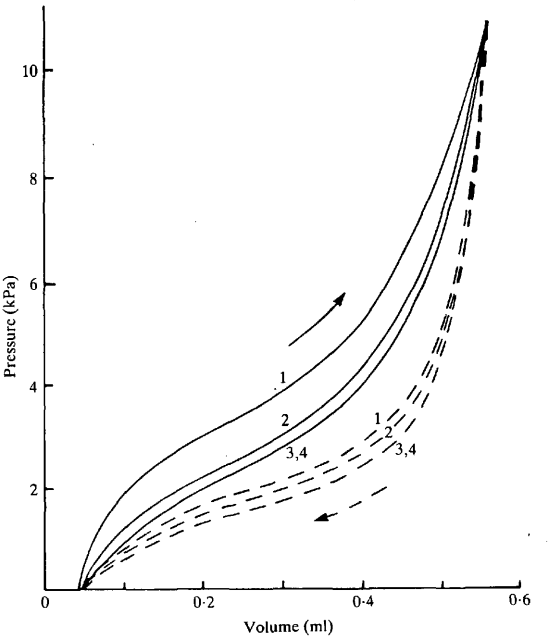

Fig. 2. Quasi-static pressure-volume curves for a segment of aorta. The inflation curves (solid lines) and deflation curves (broken lines) for the first four successive tests are shown, as indicated by the numbers, to illustrate the preconditioning phenomenon. Arrows indicate the direction of loading.

Since the product of pressure (P) and volume (V) is work, then the area under the inflation curve is the total work done (= the energy used) to distend the artery, while the area under the deflation curve is the energy recovered by elastic recoil. The area enclosed by the P-V loop is the energy lost as heat through viscous processes and, when expressed as a percentage of the total energy, is called the mechanical hysteresis. For the first inflation cycle shown in Fig. 2 the hysteresis was 43 %. With subsequent inflations the curves shifted to the right and the hysteresis loops became smaller. Three to four cycles were normally enough to obtain a stable response with about 25 % to 30 % hysteresis. The instability of hysteresis curves during the first few strain cycles is a phenomenon which is typical of arteries tested *in vitro*, and probably represents a process of internal structural readjustment to stresses after being excised and kept in an unpressurized state (Bergel, 1961*a*; Fung, 1972). The most important feature of the P-V curves is that the volume distensibility of the aorta, (dV/VdP), decreased markedly with increasing distension over the range of physiological blood pressures, approximately 2–5 kPa (Johansen & Martin, 1962).

Inflation of the octopus aorta always resulted in an increase in length as well as in circumference. The changes in these dimensions which occurred in a typical experiment are shown in Fig. 3. At a pressure of 5 kPa, the increase in length was

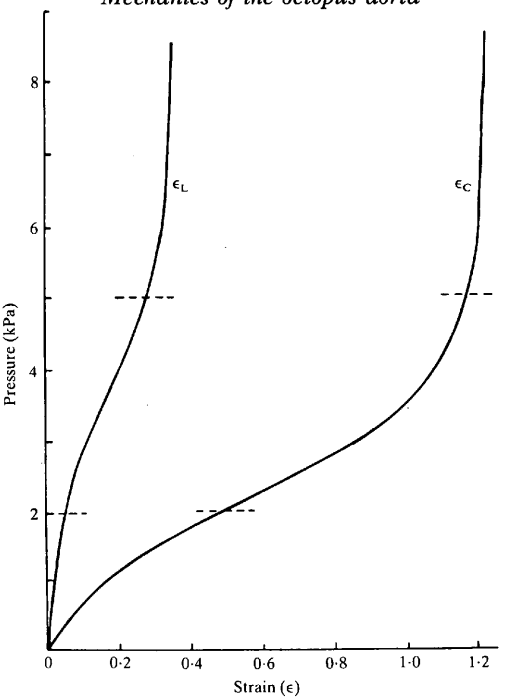

Fig. 3. Results of quasi-static pressure-volume tests, expressed in terms of the strain in circumference (ϵ_C) and in length (ϵ_L). The approximate range of physiological pressure is indicated by the broken lines.

30% ($\epsilon_L = 0{\cdot}30$), while the circumference had increased by 120% ($\epsilon_C = 1{\cdot}20$). Since luminal volume increases with the square of the radius, but only linearly with vessel length, it can be seen that circumferential strain contributes the major portion of the volume distensibility of the aorta. Above physiological pressures only relatively small changes in longitudinal and circumferential strain were observed. The aorta has a relatively thick wall at zero pressure, the ratio h/R being about 0·45 (±0·05). However, due to the large circumferential strains, at 5 kPa pressure h/R is reduced to about 0·10 (±0·01). In mammalian arteries h/R is about 0·20 at zero pressure and decreases to about half of this value at physiological pressures (Cox, 1979).

Fig. 4 presents data, taken from the inflation limb of P-V loops, in terms of stress and strain in the circumferential and longitudinal directions. The observed stress-strain relations for the octopus aorta were always non-linear. The stress-strain data for distal segments of the aorta indicate that in this region the aorta is somewhat less extensible, circumferentially and longitudinally, than the main part of the vessel which lies more proximal to the heart. While these differences in extensibility may

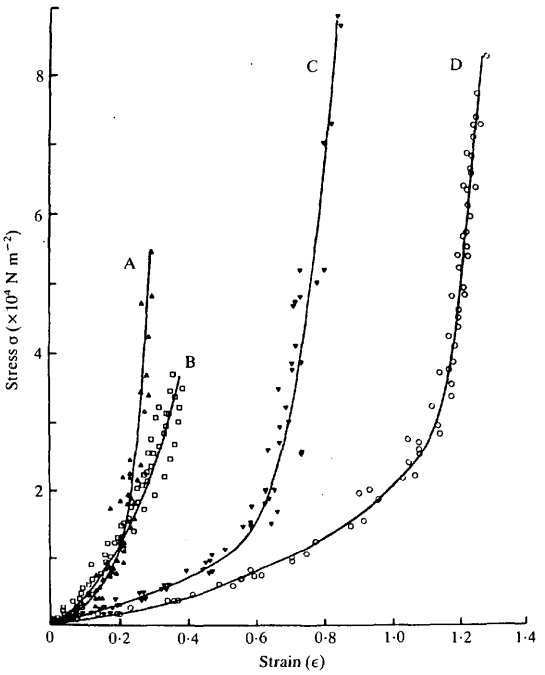

Fig. 4. Inflation data taken from ascending limb of quasi-static pressure-volume curves and computed as stress and strain in the longitudinal direction (A,B) and in the circumferential direction (C,D). Segments of aorta were taken proximal (B,D; seven samples) or distal (A,C; four samples) to the heart.

be due to an 'elastic taper' in the aorta, as occurs in the vertebrate aorta (McDonald, 1974), the possibility was not investigated further in this study. The experiments to follow deal only with the major proximal portion of the aorta which is characterized by curves B and D in Fig. 4.

Activation of vascular muscle

Immediately after excision, many aortae exhibited a brief period of spontaneous muscle activity which was severe enough to cause visible undulatory movements along the length of the vessel. However this phenomenon did not persist for more than about 30 min in cold saline. Spontaneous muscle activity was also indicated by brief, large pressure transients or by small pressure pulsations which occasionally occurred during the slow inflation of a vessel. This activity appeared to be abolished by several consecutive inflation cycles during the normal preconditioning period, or by exposure of the artery to a high pressure (10 kPa) for several minutes.

Since the main objective of this study was to measure the passive mechanical properties of the artery wall, it was necessary to be able to distinguish between the active and relaxed states of the vascular muscle. To do this, we used drugs which had previously shown excitatory or inhibitory effects on the octopus circulation *in vivo* (Johansen & Huston, 1962) or on the aorta *in vitro* (Wells & Mangold, 1980). Prolonged periods of muscle activation (i.e. several minutes) could be produced by treatment with 5-HT. Fig. 5 shows the results of an experiment in which a preconditioned aortic segment was subjected to three sets of inflations, the first with normal saline (A), the second after infusion with 5-HT (B), and the third following infusion with ACh (C). P-V curves for the control and ACh-treated artery are virtually identical. In the presence of 5-HT, however, the volume distensibility of the aorta was greatly reduced, particularly over the physiological range of pressures. Muscle activation increased hysteresis slightly above the control level (28% and 22% respectively for the example in Fig. 5). The results suggest that the muscle in preconditioned, control arteries was in the relaxed state. Thus, we can regard the results of tests on preconditioned artery samples where drugs were not used as representing the passive elastic properties of the vessel wall.

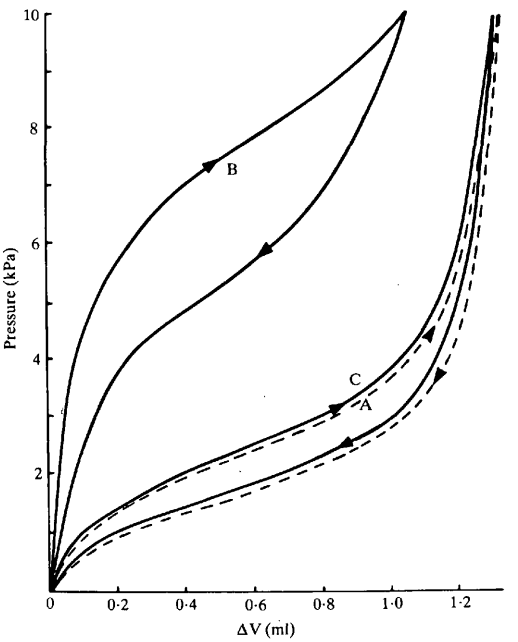

Fig. 5. Quasi-static inflation of an aortic segment under (A) control conditions, (B) following infusion of 5-hydroxytryptamine (5-HT) at 100 μg ml^{-1} concentration and (C) following infusion of acetylcholine (ACh) at 1 mg ml^{-1} concentration.

Stress-strain curves, calculated from the loading portion of P-V curves, are shown for the longitudinal and circumferential directions in Fig. 6. Here, strain is expressed with reference to the initial dimensions of the relaxed vessel. Note that 5-HT did not produce a measurable change in the external diameter at zero pressure, although the length appeared to increase by about 6%. For all strains in the octopus aorta, the circumferential and longitudinal stresses were elevated by activation of the muscle, with the exception of the initial part of the longitudinal extension. The difference between the stress curves for the stimulated and relaxed states is the active stress component, and this is shown in Fig. 6. Active stress in the circumferential direction increased continuously with strain, reaching an apparent peak at $\epsilon_C = 1{\cdot}0$. In the longitudinal direction, the active stress increased to a plateau level at $\epsilon_L > 0{\cdot}20$. These results suggest that the magnitude of the active stress response is maximal at some optimum circumference or length. This optimum dimension appears to occur at circumferential and longitudinal strains that correspond to a pressure of about 3·5 kPa, i.e. in the middle of the physiological range.

Uniaxial tests

Fig. 7 shows examples of force-extension curves obtained from quasi-static uniaxial tests of the aorta in the longitudinal and circumferential directions. We

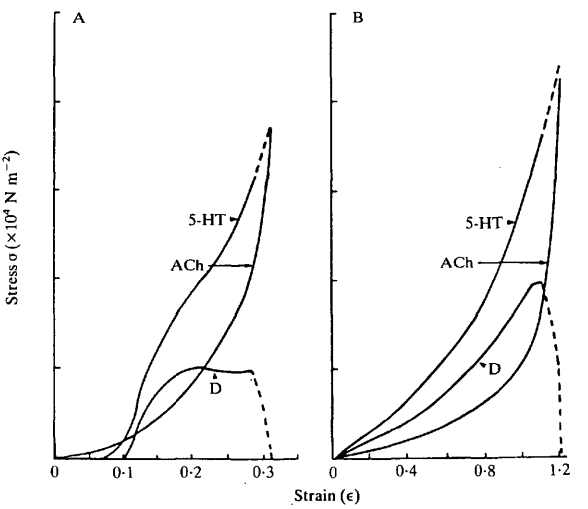

Fig. 6. Stress-strain curves computed from the loading portion of the pressure-volume curves in Fig. 5. (A) Longitudinal and (B) circumferential directions. Strain is given in terms of the initial dimensions of the relaxed vessel. Activation of muscle increased the stress in the artery wall. The 'active stress' is plotted as the difference between curves for 5-HT and ACh treatments and is labelled D. The broken part of the active stress curve is calculated by extrapolating the 5-HT curve to intersect with the ACh curve.

found that hysteresis was greater longitudinally than circumferentially (39% *vs* 26% respectively, in this case). Data from the loading portion of force-extension cycles were used to construct stress-strain curves, examples of which are plotted in Fig. 8. These curves resemble the J-shaped biaxial stress-strain curves in Fig. 4, except that the artery wall appears to be more extensible, for a given stress, when loaded uniaxially than biaxially. This difference was expected according to equations 9 and 10, and was most noticeable in the circumferential direction.

Values of the tangential elastic moduli, E_L and E_C, were calculated from uniaxial stress-strain data using equation 1 (Fig. 9). Over the range of extensions used the artery wall increased in stiffness by approximately two orders of magnitude: E_L varied from 3×10^3 to $1{\cdot}8\times10^5\,N\,m^{-2}$, while E_C varied from about 5×10^3 to $5\times10^5\,N\,m^{-2}$. These values of modulus are characteristic of an elastic material which has from 1/200 to 1/2 the stiffness of an ordinary rubber band. The large increase in elastic modulus which accompanies increasing strain explains the decreased volume distensibility observed at high pressures (Fig. 2).

Calculation of E_C from inflation data

Uniaxial tests on isolated artery rings are simple and convenient, but the results from these tests may be unreliable at very high strains where fibre orientations within the vessel wall must differ considerably between uniaxial and biaxial specimens. Therefore we wanted to calculate the circumferential elastic modulus from biaxial inflation data. This requires the knowledge of either Poisson's ratio or the longitudinal modulus. Since Poisson's ratios were not measured directly, we decided to use values of E_L from uniaxial tests in order to determine ν_{CL} and E_C from

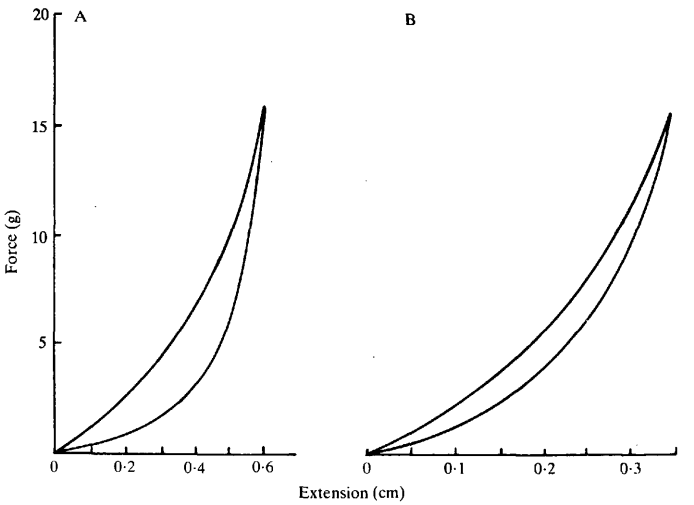

Fig. 7. Typical hysteresis curves obtained from quasi-static uniaxial tests of the aorta. (A) Longitudinal and (B) circumferential directions. Hysteresis is 39% in (A) and 26% in (B).

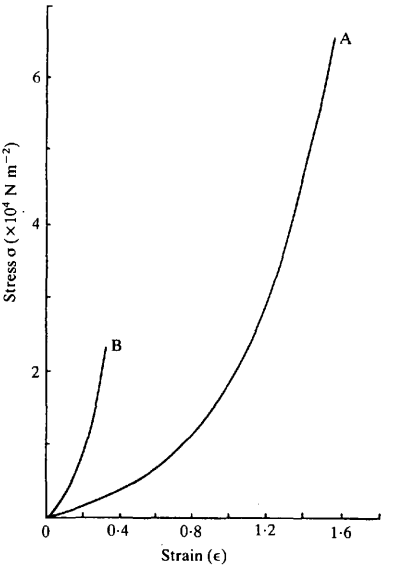

Fig. 8. Examples of stress-strain curves calculated from uniaxial tests in (A) circumferential and (B) longitudinal directions.

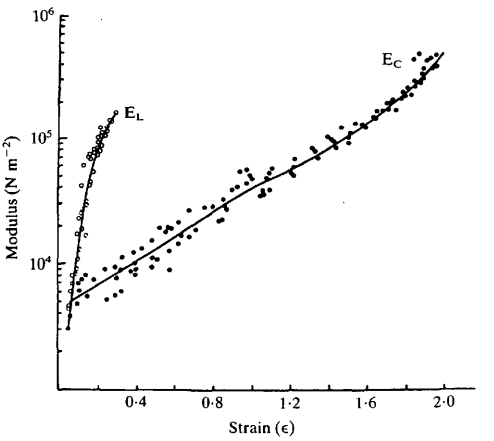

Fig. 9. Tangential elastic moduli, E_L and E_C calculated from uniaxial stress-strain data by equation 1 (samples of 6 and 10 aortae respectively). Modulus is plotted on a logarithmic scale as a function of linear strain. Curves were fitted by polynomial regression analysis.

the biaxial data. To do this, we assumed that the uniaxial E_L values are close to the true biaxial values. The assumption is reasonable since the longitudinal uniaxial tests involved only small strains (up to 30%) which presumably did not cause too extensive an alteration in fibre orientation.

Values of ν_{CL} calculated from equation 9, varied from 0·20 to 0·54 with a mean of 0·30. We used these values to determine E_C by solving equation 10. E_C is plotted as a function of pressure in Fig. 10, and as a function of strain in Fig. 11. E_C increased from 9×10^3 to $2{\cdot}3\times10^5$ N m^{-2}, over the approximate physiological pressure range, which corresponds to circumferential strains of 0·5 to 1·18 respectively. The ratio of the moduli, E_C/E_L, varied between 1·05 and 3·30 (Fig. 10). It appears that the octopus aorta has greater stiffness circumferentially than longitudinally at all pressures, and has a Poisson's ratio which is generally less than 0·5. Under these conditions equation 9 yields positive values of $\Delta\epsilon_L$: that is, the artery should lengthen as it is inflated.

The curve for E_C obtained from uniaxial tests (Fig. 9) is redrawn in Fig. 11 for comparison with E_C values determined from inflation tests. For strains below 1·10, tests on artery rings yielded values of E_C which are in close agreement with those obtained from inflation of vessel segments. At strains above 1·10 the two curves

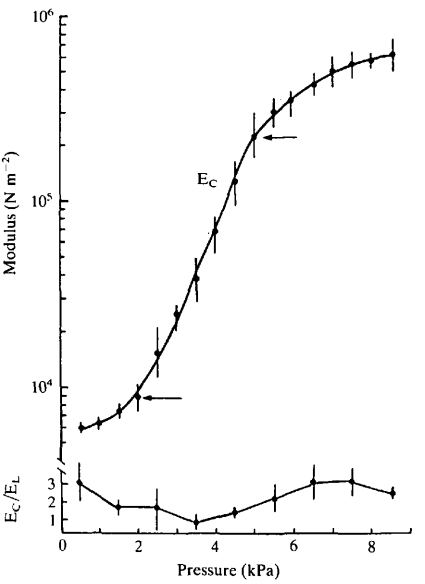

Fig. 10. Circumferential modulus of elasticity, E_C, plotted as a function of inflation pressure. The ratio of circumferential modulus to longitudinal modulus (E_C/E_L) is also shown. Points represent means from seven samples, and bars are ± one standard error. The approximate physiological blood pressure range is indicated by the arrows.

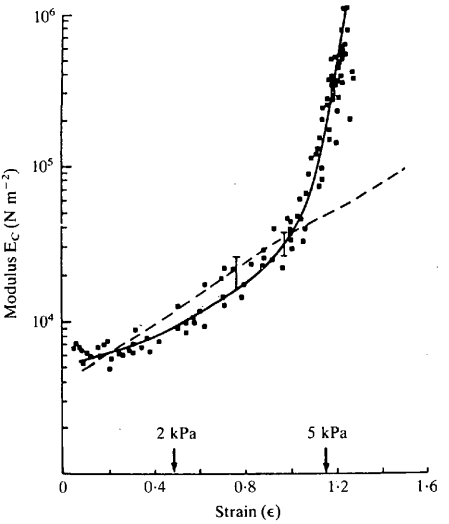

Fig. 11. Circumferential elastic modulus E_C as a function of strain. The data points and corresponding polynomial regression curve (solid line) were calculated from biaxial inflation data (seven samples) using equations 9 and 10. Vertical bars are one standard deviation. The broken line represents E_C, as calculated from uniaxial stress-strain data, and has been redrawn from Fig. 9. Arrows on the abcissa show the approximate strains for pressures of 2 and 5 kPa.

diverge. The ring samples may be expected to show mechanical behaviour which is different from the intact vessel, particularly at high extensions, because the artery wall is not a homogeneous material. At large strains it is likely that fibre networks in the artery wall will be considerably reorientated, in ways which may differ in the two types of samples. Since these analytical methods are not exact, the results must be regarded as only approximations of the true values. It is quite satisfying, therefore, that uniaxial and biaxial tests on the aorta gave similar values of E_C for strains which include the physiological range. This indicates that uniaxial tests on ring samples are legitimate for extensions up to about 100%.

Viscoelastic properties

The presence of a significant viscous component in the mechanical response of octopus artery wall was indicated by hysteresis in the quasi-static inflations. Other viscoelastic phenomena which we observed during step-wise inflation of the aorta were stress-relaxation and creep (data not shown). Since arterial viscoelasticity is important in determining haemodynamic relationships, we decided to characterize this property by dynamic testing.

A quantitative analysis of the frequency-dependent mechanical properties of the octopus aorta is based on the combined results of dynamic mechanical tests on intact vessel segments and ring samples. In these tests small sinusoidal strain oscillations

were superimposed on different levels of pre-strain (Fig. 12A). Examples of a pressure-radius loop from a dynamic inflation experiment (Fig. 12B) and a force-extension loop from an artery ring vibration test are given (Fig. 12C). Both show that the strain increments were sufficiently small that these loops were approximately linear. Fig. 13A shows that the storage modulus E′ increased continuously with the frequency of oscillation for each level of pre-strain which was tested. In addition, the proportional change in E′ over the range of frequencies used increased with strain, i.e. the ratio of E′ at 10 Hz to E′ at 0·1 Hz was 1·33 at $\epsilon_C = 0{\cdot}3$ (curve d), 1·43 at $\epsilon_C = 0{\cdot}6$ (curve c), 1·88 at $\epsilon_C = 1{\cdot}0$ (curve b) and 1·96 at $\epsilon_C = 1{\cdot}2$ (curve a).

In all experiments, the phase angle δ was positive, i.e. the change in pressure (or force) always led the change in radius (or extension), and tan δ varied between 0·11 and 0·27 (Fig. 13B). For these values of tan δ, E′ is approximately equal to E* and E″ is relatively small. Unlike E′, tan δ did not seem to change significantly with different levels of pre-strain, except perhaps at the highest frequencies when curves for higher pre-strain (a and b) appear to diverge from curves for lower pre-strain (c and d). With increasing frequency there was a steady rise in tan δ, suggesting that the loss modulus E″ was increasing relative to E′ (since $\tan\delta = E''/E'$). However, the large scatter in data at frequencies above 1 Hz may indicate that errors were being introduced due to inertial effects of fluid acceleration in the vessel. We were unable to assess to what extent this problem influenced our measurements.

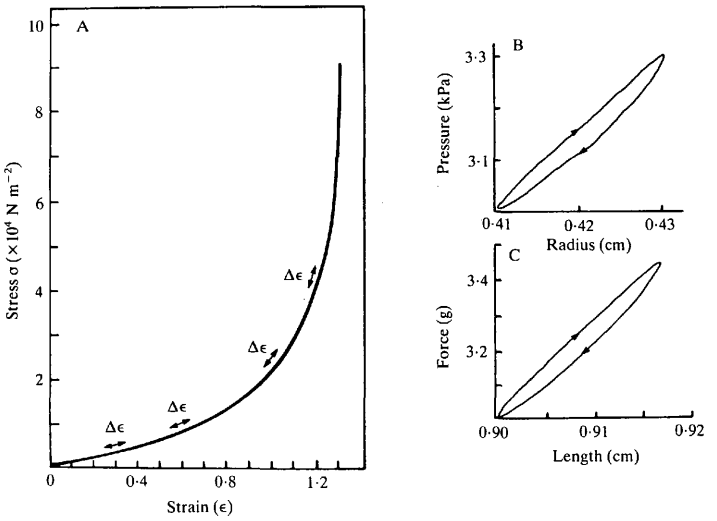

Fig. 12. Diagram to illustrate dynamic mechanical testing of the aorta. Small sinusoidal oscillations of strain were imposed at four levels of pre-strain, as shown in (A). (B) A pressure-radius loop from a dynamic inflation experiment, and (C) a force-length loop from a vibration test, both done at a frequency of 1 Hz.

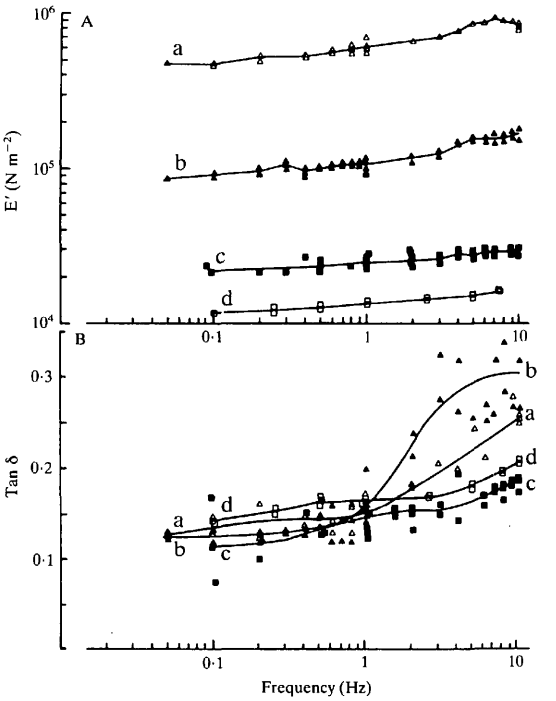

Fig. 13. Results of dynamic mechanical tests on the aorta, showing (A) storage modulus E′ and (B) loss tangent tan δ plotted as functions of frequency. Four levels of pre-strain (ϵ_C) were used: (a) $\epsilon_C = 1{\cdot}2$, mean pressure = 6 kPa; (b) $\epsilon_C = 1{\cdot}0$, mean pressure = 4 kPa; (c) $\epsilon_C = 0{\cdot}6$, mean pressure = 3 kPa; (d) $\epsilon_C = 0{\cdot}3$. Sample sizes of 4, 5, 6 and 3 respectively.

We defined the mechanical hysteresis to be the energy lost expressed as a percentage of the total energy used through one cycle of deformation. The efficiency of elastic energy storage may be expressed as the resilience Re, which is defined as the percentage of total energy input that is recovered in elastic recoil. Re = 100−H, where H is the hysteresis. In the quasi-static tests (Fig. 2) the octopus aorta exhibited hysteresis of about 25 % to 30 %, corresponding to a resilience of 75 % to 70 %. In viscoelastic materials the resilience usually decreases with increasing frequency. Since tan δ is proportional to the ratio of energy lost to energy stored in one cycle of a sinusoidal oscillation, the hysteresis may be calculated as (Wainwright *et al.* 1976):

$$\frac{\mathrm{Re}}{100} = \exp(-\pi \tan \delta). \tag{16}$$

In dynamic tests at a mean strain of 1·0, Re was 70 % at 0·05 Hz (tan $\delta = 0{\cdot}11$), 67 % at 0·5 Hz (tan $\delta = 0{\cdot}13$) and 62 % at 1·0 Hz (tan $\delta = 0{\cdot}15$). Physiologically

relevant frequencies of pressure oscillations in the aorta of *O. dofleini* range up to about 1·0 Hz (R. E. Shadwick & J. M. Gosline, in preparation). At frequencies above 1·0 Hz, tan δ continued to increase, (Fig. 13B, curve b), with a concomitant drop in the elastic energy storage efficiency.

DISCUSSION

Quasi-static mechanical properties

The results of this study show that the octopus aorta is a highly distensible and resilient elastic vessel which is well suited to function as an elastic reservoir in the central circulation. A very important feature of the aorta is that the elasticity is highly non-linear. Over the physiological pressure range the passive distensibility of the vessel wall changed dramatically as the circumferential elastic modulus increased from a relatively low value of about 10^4 up to about 2×10^5 N m^{-2}. Thus, a twenty-fold increase in stiffness occurs over the range of strain imposed on the artery wall by a resting blood pressure pulse. Similarly, in other cephalopods we found large changes in the aortic wall stiffness with extension in the physiological pressure range. In the nautilus (*Nautilus pompilius*) E_C increased from 2×10^4 to 2×10^5 N m^{-2} between pressures of 2 and 6 kPa respectively, while in the squid (*Nototodarus sloani*) E_C increased from 10^5 to 10^6 N m^{-2} between pressures of 10 and 20 kPa respectively (Gosline & Shadwick, 1982).

Non-linear elasticity is also characteristic of vertebrate arteries. For example, Bergel (1961*a*) showed that the luminal volume of the canine thoracic aorta increased by about four times when inflated from 0 to 40 kPa pressure, and the circumferential elastic modulus increased from 2×10^5 to about 10^6 N m^{-2} between 11 and 22 kPa, the approximate *in vivo* blood pressure. All blood vessels that have been studied exhibit 'J-shaped' stress-strain curves and a progressive increase in wall stiffness with extension, or pressure (Bergel, 1961*a*; Cox, 1979; Fung, 1981). Apparently this is a design feature of highly distensible pressure vessels which is necessary in order to prevent instability and rupture (Burton, 1954; Gordon, 1975; Bogen & McMahon, 1979).

Burton (1954) showed that for a pressurized elastic tube the volume distensibility D (= dV/VdP), is inversely proportional to [(Eh/R)−P], where E is the elastic modulus, h is the wall thickness, R is the radius and P is the pressure. As the pressure is raised, R will increase and h will decrease. If E remains constant with extension, then D will become infinitely large as P approaches Eh/R, and the tube will rupture. This can be avoided either by having E very large relative to P, or by having E increase with radius, such that Eh/R is always greater than P. In the first case the tube would be non-compliant (e.g. a steel water pipe), but this would not be useful as an elastic reservoir. The second case is what has been observed for the arteries of vertebrates as well as cephalopods. This allows the vessel to have large compliance at low pressures, thereby smoothing the pulse and offering low resistance to flow from the heart, and yet still be protected from 'blowout' at higher pressures. The range of modulus which is necessary to meet the above criteria will depend on the physiological pressures normally experienced, and on the dimensions of the vessel. The elastic modulus of the aorta is lower in the relatively low pressure

circulatory systems of octopus and nautilus than in the high pressure systems of squid and dog.

In our experiments the artery segments were free to lengthen when inflated, so as to mimic the situation in the animal. The octopus has no rigid skeleton, so the aorta cannot be tethered to a fixed length *in vivo*. In contrast, the vertebrate aorta is restricted longitudinally by the axial skeleton, and retracts by about 30% when excised (Dobrin, 1978). The length change that occurs when the vessel is inflated depends on the Poisson's ratios and the relative stiffness in the circumferential and longitudinal directions (equations 8, 9). E_C was greater than E_L at all pressures in the octopus aorta. The vessel lengthened when inflated, although the longitudinal strain was always less than the circumferential strain. Mechanical anisotropy has also been demonstrated in many mammalian arteries. Patel, Janicki & Carew (1969) found that E_L was greater than E_C in the dog thoracic aorta. Others have shown that E_C is greater than E_L in the dog carotid artery (Dobrin & Doyle, 1970; Cox, 1975).

The passive hysteresis for slow inflation of the octopus aorta was slightly greater than that typically observed in mammalian arteries. Vascular muscle is the main factor contributing to hysteresis in the artery wall (Dobrin, 1978), although a small amount of hysteresis is also found in isolated elastin and collagen when tested at low strain rates (Fung, 1981). The octopus aorta has more muscle, and less collagen and elastic fibres than have mammalian arteries (Shadwick & Gosline, 1983). These differences in composition of the tissue components, as well as their structural organization, probably account for the lower elastic modulus and greater hysteresis in the aorta of the octopus *versus* the mammal.

Hysteresis is increased by activation of the muscle component in mammalian arteries (Dobrin, 1973; Busse, Bauer, Sattler & Schabert, 1981) and apparently in the octopus aorta as well. We do not fully understand the role of the muscle in the octopus vessel wall. Fibroblast cells must be responsible for the deposition of the extracellular connective tissues. Muscle cells may serve this purpose, as well as forming a mechanical linkage between fibres in the elastic network (Shadwick & Gosline, 1983). Vascular muscle may be responsible for active propulsion of blood through the circulation, but this has not been clearly demonstrated (Johansen & Martin, 1962; Wells, 1978). It seems unlikely that muscle activation in the aorta could be important in regulating blood flow resistance since this parameter must be influenced predominantly by the peripheral vessels.

Structural basis of non-linear elasticity

The non-linear elastic properties of the mammalian artery wall are attributed to the parallel arrangement of elastin and collagen fibre systems. Elastin itself has non-linear elasticity because of its non-Gaussian behaviour (Aaron & Gosline, 1981). However, the increase in stiffness of isolated elastin fibres with extension is not nearly as great as the increase in stiffness which occurs with comparable strains in the whole artery wall. Thus, the 'J' shape of the stress-strain curve for the mammalian artery arises, not from the non-linear properties of elastin, but from the recruitment of more elastin fibres and the transfer of load to the collagen network, as the artery is inflated (Roach & Burton, 1957; Wolinsky & Glagov, 1964).

In contrast, the non-linear elasticity of the OAE fibres may be important in determining the shape of the stress-strain curve for the octopus aorta. It was shown in the previous paper (Shadwick & Gosline, 1985) that the molecular chains of the OAE protein are more restricted in their flexibility than are those of elastin. Consequently, the stiffness of the OAE fibres increases rapidly with stretch in the region of non-Gaussian extensions. In Fig. 14 the shapes of the stress-strain curves for the octopus artery wall and for the OAE fibres are compared. Here, the stress scales have been adjusted arbitrarily so that the initial portions of the curves coincide (up to $\epsilon = 0{\cdot}2$). When this is done, it can be seen that the curves are almost identical in form up to strains of 1·2. By this semi-quantitative method it appears that the non-Gaussian behaviour of the elastic fibres gives rise to an increase in stiffness, with extension, which is similar to the non-linear elasticity of the whole artery wall, up to and including the normal range of physiological extensions.

We found that the elastic fibre network comprises about 3 % of the volume of the aorta, and that the fibres are present as a sheet lining the vessel lumen, and as a multi-directional array throughout the muscle layers (Shadwick & Gosline, 1983, 1985). Fig. 14 shows that up to $\epsilon = 1{\cdot}2$ the stress required to stretch the elastic fibres is about 100 times greater than the circumferential stress in the whole artery wall (i.e. the stress scales in Fig. 14 differ by a factor of about 100). If as little as one-third of the total fibre content (i.e. about 1 % of the wall material) is orientated to support the circumferential stress when the artery is inflated, then the presence of elastic fibres alone can account for the stiffness of the artery wall through the physiological range of pressures. Collagen, which is present as a loose adventitia, may not be required to take a significant portion of the load until very large extensions.

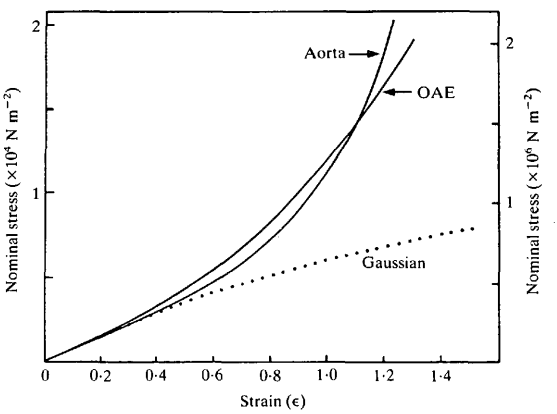

Fig. 14. Curves of nominal stress *vs* strain for the octopus aorta (circumferential direction), for the octopus arterial elastomer (OAE), and for a Gaussian rubber with the same elastic modulus as the OAE. Left ordinate is for the aorta; right ordinate is for the OAE and the rubber. Stress scales are adjusted so that the curves coincide up to a strain of 0·2. Nominal stress = true stress/(1 + strain.)

The octopus aorta as an elastic reservoir

The results of our dynamic mechanical tests show that the octopus aorta is a viscoelastic structure which becomes stiffer and less resilient with increasing rates of deformation. E′ and tan δ both increased continuously with frequency over the range of 0·05 to 10 Hz. This type of behaviour is typical of other biomaterials and polymeric solids at frequencies below the glass transition (Ferry, 1970; Fung, 1981). In the mammalian artery wall E′ increases by up to twice the quasi-static value, and tan δ generally rises from about 0·09 to 0·20 with frequencies from 0·2 to 20 Hz respectively (Bergel, 1961*b*; Gow, 1970; Patel, Janicki, Vaishnav & Young, 1973; Busse *et al.* 1981). The magnitude of viscosity in mammalian arteries can be correlated with the amount of vascular muscle at different anatomical sites, as can hysteresis and stress relaxation properties (Dobrin, 1978). In terms of tan δ and the relative change in E′ between 0 and 10 Hz, the octopus aorta is comparable to the carotid artery of mammals. No data are available for the dynamic mechanical properties of any other cephalopod arteries.

Viscous energy losses in the artery wall decrease the efficiency of elastic energy storage in the system. However, some degree of wall viscosity may be haemodynamically favourable. The impedance to flow which the heart must work against is determined by a complex interaction between incident and reflected pressure waves in the arterial tree; wall viscosity causes attenuation of pressure waves, and this can reduce the impedance (Taylor, 1966). Since viscosity in the artery wall arises primarily from the muscle component, then the amount of muscle present in an artery may be determined, at least in part, by a mechanical requirement to optimize elastic recoil and pressure wave damping in the vessel wall.

In the physiological range of frequencies for *Octopus dofleini* (about 0·1 to 1 Hz) the resilience of the aorta varied from 70 % to 62 %. This is only slightly less than the resilience of the mammalian aorta at the relevant physiological frequencies (approx. 2–20 Hz in the dog; Bergel, 1961*b*). Thus the octopus aorta appears to have mechanical properties which would allow it to function effectively as an elastic reservoir in the circulatory system. We are currently investigating the relationship between arterial mechanical properties and the fluid dynamics of blood flow in the living octopus.

This research was funded by an operating grant to JMG from NSERC of Canada.

REFERENCES

AARON, B. B. & GOSLINE, J. M. (1981). Elastin as a random-network elastomer: a mechanical and optical analysis of single elastin fibres. *Biopolymers* **20**, 1247–1260.

ATTINGER, F. M. L. (1968). Two-dimensional *in vitro* studies of femoral arterial walls of the dog. *Circulation Res.* **22**, 829–840.

BERGEL, D. H. (1961*a*). Static elastic properties of the arterial wall. *J. Physiol., Lond.* **156**, 445–457.

BERGEL, D. H. (1961*b*). Dynamic elastic properties of the arterial wall. *J. Physiol., Lond.* **156**, 458–469.

BERGEL, D. H. (1972). The properties of blood vessels. In *Biomechanics*, (eds Y. C. Fung, N. Peronne & M. Anliker), pp. 105–139. New Jersey: Prentice-Hall.

BOGEN, D. K. & MCMAHON, T. A. (1979). Do cardiac aneurysms blow out? *Biophys. J.* **27**, 301–316.

BOURNE, G. B. (1982). Blood pressure in the squid *Loligo pealei*. *Comp. Biochem. Physiol.* **72A**, 23–27.

BOURNE, G. B., REDMOND, J. R. & JOHANSEN, K. (1978). Some aspects of hemodynamics in *Nautilus pompilius*. *J. exp. Zool.* **205**, 63–70.

BROWNING, J. (1980). The vasculature of *Octopus* arms: a scanning electron microscope study of corrosion casts. *Zoomorph.* **96**, 243–253.

BURGGREN, W. (1977). The pulmonary circulation of the chelonian reptile: morphology, hemodynamics and pharmacology. *J. comp. Physiol.* **116**, 303–323.

BURTON, A. C. (1954). Relation of structure to function of the tissue of the walls of blood vessels. *Physiol. Rev.* **34**, 619–642.

BUSSE, R., BAUER, R. D., SATTLER, T. & SCHABERT, A. (1981). Dependence of elastic and viscous properties on circumferential wall stress at two different smooth muscle tones. *Pflügers Arch. ges. Physiol.* **390**, 113–119.

COX, R. H. (1975). Anisotropic properties of the canine carotid artery *in vitro*. *J. Biomech.* **8**, 293–300.

COX, R. H. (1979). Physiology and hemodynamics of the macrocirculation. In *Hemodynamics and the Blood Vessel Wall*, (ed. W. E. Stehbens). Springfield, Ill.: C. C. Thomas.

DENNY, M. W. & GOSLINE, J. M. (1980). The physical properties of the pedal mucus of the terrestrial slug *Ariolimax columbianus*. *J. exp. Biol.* **88**, 375–394.

DOBRIN, P. B. (1973). Influence of initial length on length-tension relationship of vascular smooth muscle. *Am. J. Physiol.* **225**, 664–670.

DOBRIN, P. B. (1978). Mechanical properties of arteries. *Physiol. Rev.* **58**, 397–460.

DOBRIN, P. B. & DOYLE, J. M. (1970). Vascular smooth muscle and the anisotropy of dog carotid artery. *Circulation Res.* **27**, 105–119.

FERRY, J. D. (1970). *Viscoelastic Properties of Polymers*. New York: Wiley.

FUNG, Y. C. (1972). Stress-strain history relations in soft tissues in simple elongation. In *Biomechanics*, (eds Y. C. Fung, N. Peronne & M. Anliker), pp. 181–208. New Jersey: Prentice-Hall.

FUNG, Y. C. (1981). *Biomechanics. Mechanical Properties of Living Tissues*. New York: Springer-Verlag.

GABE, I. T. (1972). Pressure measurement in experimental physiology. In *Cardiovascular Fluid Dynamics*, Vol. 1, (ed. D. H. Bergel), pp. 11–50. New York: Academic Press.

GOEDHARD, W. J. A. & KNOOP, A. A. (1973). A model of the arterial wall. *J. Biomech.* **6**, 281–288.

GORDON, J. E. (1975). Mechanical instabilities in biological membranes. In *Comparative Physiology. Functional Aspects of Structural Materials*, (eds L. Bolis, S. H. P. Maddrell & K. Schmidt-Nielsen), pp. 49–57. Amsterdam: North Holland.

GOSLINE, J. M. & FRENCH, C. J. (1979). Dynamic mechanical properties of elastin. *Biopolymers* **18**, 2091–2103.

GOSLINE, J. M. & SHADWICK, R. E. (1982). The biomechanics of cephalopod arteries. *Pacific Science* **36**, 283–296.

GOW, B. S. (1970). Viscoelastic properties of conduit arteries. *Circulation Res. (Suppl.)* **II**, 113–122.

JOHANSEN, K. & HUSTON, M. J. (1962). Effect of some drugs on the circulatory system in the intact, non-anaesthetized cephalopod *Octopus dofleini*. *Comp. Biochem. Physiol.* **5**, 177–184.

JOHANSEN, K. & MARTIN, A. W. (1962). Circulation in the cephalopod *Octopus dofleini*. *Comp. Biochem. Physiol.* **5**, 161–176.

LANGILLE, B. L. & JONES, D. R. (1975). Central cardiovascular dynamics of ducks. *Am. J. Physiol.* **228**, 1856–1861.

LANGILLE, B. L. & JONES, D. R. (1977). Dynamics of blood flow through the hearts and arterial systems of anuran amphibia. *J. exp. Biol.* **68**, 1–17.

MCDONALD, D. A. (1974). *Blood Flow in Arteries*. London: Edward Arnold.

PATEL, D. J., JANICKI, J. S. & CAREW, T. E. (1969). Static anisotropic elastic properties of the aorta in living dogs. *Circulation Res.* **25**, 765–779.

PATEL, D. J., JANICKI, J. S., VAISHNAV, R. N. & YOUNG, J. T. (1973). Dynamic anisotropic viscoelastic properties of the aorta in living dogs. *Circulation Res.* **32**, 53–107.

ROACH, M. R. & BURTON, A. C. (1957). The reason for the shape of the distensibility curves of arteries. *Can. J. Biochem. Physiol.* **35**, 681–690.

ROY, C. S. (1880). The elastic properties of the arterial wall. *J. Physiol., Lond.* **3**, 125–162.

SATCHELL, G. H. (1971). *Circulation in Fishes*. Cambridge Monographs in Experimental Biology No. 18 (131 pp.). Cambridge: Cambridge University Press.

SHADWICK, R. E. & GOSLINE, J. M. (1981). Elastic arteries in invertebrates: mechanics of the octopus aorta. *Science, N.Y.* **213**, 759–761.

SHADWICK, R. E. & GOSLINE, J. M. (1983). The structural organisation of an elastic fibre network in the aorta of the cephalopod *Octopus dofleini*. *Can J. Zool.* **61**, 1866–1879.

SHADWICK, R. E. & GOSLINE, J. M. (1985). Physical and chemical properties of rubber-like elastic fibres from the octopus aorta. *J. exp. Biol.* **114**, 239–257.

SPECKMAN, E. W. & RINGER, R. K. (1966). Volume pressure relationships in the turkey aorta. *Can. J. Physiol. Pharmacol.* **44**, 901.

TAYLOR, M. G. (1966). The input impedance of an assembly of randomly branching elastic tubes. *Biophys. J.* **6**, 29–51.

WAINWRIGHT, S. A., BIGGS, W. D., CURREY, J. D. & GOSLINE, J. M. (1976). *Mechanical Design in Organisms*. London: Edward Arnold.

WELLS, M. J. (1978). *Octopus: Physiology and Behaviour of an Advanced Invertebrate*, (440 pp). London: Chapman & Hall.

WELLS, M. J. (1979). The heartbeat of *Octopus vulgaris*. *J. exp. Biol.* **78**, 87–104.

WELLS, M. J. (1983). Circulation in cephalopods. In *The Mollusca*, Vol. 5, *Physiology*, pp. 239–290. New York: Academic Press.

WELLS, M. J. & MANGOLD, K. (1980). The effects of extracts from neurosecretory cells in the anterior vena cava and pharyngeophthalmic vein upon the hearts of intact free moving octopuses. *J. exp. Biol.* **84**, 319–334.

WOLINSKY, H. & GLAGOV, S. (1964). Structural basis for the static mechanical properties of the aortic media. *Circulation Res.* **14**, 400–413.